

See discussions, stats, and author profiles for this publication at: <https://www.researchgate.net/publication/47697968>

Lipid-Induced Calcitonin Fibrillation Blocks Membrane Interactions of a Peptide Antibiotic

ARTICLE *in* THE JOURNAL OF PHYSICAL CHEMISTRY B · NOVEMBER 2010

Impact Factor: 3.3 · DOI: 10.1021/jp1072473 · Source: PubMed

CITATIONS

2

READS

21

2 AUTHORS, INCLUDING:



Tania Sheynis

University of Leeds

25 PUBLICATIONS 418 CITATIONS

SEE PROFILE

Lipid-Induced Calcitonin Fibrillation Blocks Membrane Interactions of a Peptide Antibiotic

Tania Sheynis and Raz Jelinek*

Department of Chemistry, Ben-Gurion University of the Negev, Beer-Sheva 84105, Israel

Received: August 2, 2010; Revised Manuscript Received: September 13, 2010

Interactions between membranes and amyloid proteins are believed to be a major factor contributing to pathogenesis in amyloid diseases. Furthermore, membranes have been shown to closely affect fibrillation processes of varied amyloidogenic peptides. Here we describe an intriguing phenomenon in which bilayer-induced fibrillation of human calcitonin (hCT) gave rise to significant inhibition of membrane interactions of alamethicin, an antibiotic, membrane-permeating peptide. This “membrane shielding” effect was apparent only when fibrillation of hCT occurred in the presence of cholesterol-containing vesicles; no interference with membrane binding was detected when hCT fibrillar species were formed in noncholesterol lipid environments, or when hCT amyloid aggregates were separately added to lipid bilayers. The experimental data indicate that cholesterol-promoted formation of amyloid fibril network at the bilayer interface is most likely responsible for the shielding effect. This phenomenon might point to a role of amyloid fibers in preventing membrane disruption by antibiotic peptides and other toxic species.

Introduction

Membrane interactions of amyloidogenic proteins appear to constitute an important biological factor in amyloid diseases. Varied amyloid-related membrane- and lipid-associated phenomena have been reported in recent years, including the formation of amyloid-induced pores and ion channels in membranes,^{1–4} lipid-promoted fibrillation,^{5–7} membrane-induced inhibition of amyloidogenesis,⁸ and others. Despite the intense interest in this field, there has not yet emerged a rigorous description as to the fundamental significance of membrane association and interactions by amyloidogenic peptides. Furthermore, in accordance with the striking similarity of fibrillar structures associated with different amyloidogenic proteins and diseases, it is apparent that membrane interactions play similar roles for different amyloidogenic protein families.

The majority of investigations into membrane interactions of amyloidogenic proteins have focused on two main aspects: on the one hand, characterizing the interactions of fibrillar species (monomers, oligomers, mature fibrils) with bilayers and the biological relevance and implication of such interactions, and on the other hand, the effects of membranes upon fibrillation phenomena involving amyloidogenic peptides. Here we examine a different concept: the effect of lipid-induced peptide fibrillation upon the subsequent bilayer interactions of other membrane-associated molecules. Specifically, we show that membrane-induced fibrillation of human calcitonin (hCT) results in significant attenuation of bilayer interactions of membrane-active peptides.

hCT is a 32-residue peptide hormone which participates in calcium–phosphorus metabolism.⁹ Due to its inhibitory activity of bone resorption, calcitonin is used as a therapeutic agent in various bone disorders, including osteoporosis¹⁰ and Paget’s disease.¹¹ hCT also exhibits marked tendency to form amyloid fibrils, which have been identified both *in vivo* and *in vitro*.^{12–14} Interestingly, hCT forms both intracellular and extracellular amyloid aggregates associated with medullary thyroid carcinoma^{13–16} and

serves as efficient marker of this type of cancer.¹⁷ However, there is evidence that aggregated forms of hCT are also secreted into serum in healthy subjects.^{12,18}

Similar to known amyloid protein systems, calcitonin forms various intermediate species throughout the aggregation process, including annular oligomers and protofibrils.¹⁹ Calcitonin aggregates were also shown to exhibit membrane interactions. In particular, biophysical analyses pointed to the formation of calcitonin-induced oligomeric pores in lipid bilayers.^{20,21} Importantly, several studies have demonstrated that the presence of lipid bilayers and their lipid compositions significantly modulated calcitonin fibril kinetics and fiber morphologies.^{22,23} In particular, it was shown that the peptide binds with high affinity to membranes that contained cholesterol or gangliosides,⁷ and moreover incubation of calcitonin with ganglioside- and cholesterol-rich membranes resulted in pronounced amyloidogenic fibrillar structures.⁷

This study examines the consequences of lipid-induced hCT fibrillation in the context of lipid bilayer properties. Specifically, the experiments were designed to evaluate whether the fibrillation process of hCT affected interaction of other membrane-active peptides. To probe membrane interactions of both the hCT species (monomers, oligomers, and fibrillar aggregates) and the representative membrane-active peptide alamethicin,^{24–27} we employed several complementary biophysical techniques: lipid/polydiacetylene (PDA) vesicle assay is a recently developed assay for probing the occurrence and extent of bilayer interactions of membrane-active substances.^{28–31} Fluorescence resonance energy transfer (FRET) has been used to measure the impact of membrane interactions upon energy transfer between fluorescence donor and acceptor molecules embedded in lipid bilayers,^{32,33} while fluorescence quenching analysis has been applied to probe binding of soluble species to bilayer interfaces.^{34,35}

Experimental Section

Materials. Human calcitonin was purchased in lyophilized form at $\geq 97\%$ purity (HPLC) from Calbiochem (Merck Group, Darmstadt, Germany). Alamethicin from *Trichoderma viride*

* To whom correspondence should be addressed. Phone: (+972)86472583. Fax: (+972)86472943. E-mail: razj@bgu.ac.il.

was obtained at $\geq 98\%$ purity confirmed by HPLC from Sigma-Aldrich (St. Louis, MO). 1,2-Dimyristoyl-*sn*-glycero-3-[phospho-*rac*-(1-glycerol)] (DMPG), sphingomyelin, cholesterol, 1,2-dipalmitoyl-*sn*-glycero-3-phosphoethanolamine-*N*-(7-nitro-2-1,3-benzoxadiazol-4-yl), ammonium salt (NBD-PE); 1,2-dipalmitoyl-*sn*-glycero-3-phosphoethanolamine-*N*-(lissamine rhodamine B sulfonyl), ammonium salt (rhodamine-PE) were purchased from Avanti Polar Lipids (AL). The diacetylenic monomer, 10,12-tricosadiynoic acid, was purchased from GFS Chemicals (Powell, OH), washed in chloroform, and filtered through a $0.45\ \mu\text{m}$ nylon filter prior to use.

Vesicle Preparation. All lipid constituents were dissolved in chloroform/ethanol (1:1 v/v) and dried in vacuo to constant weight. PDA-based vesicles composed of sphingomyelin/PDA (2/3 mol ratio) and sphingomyelin/cholesterol/PDA (1/1/3 mol ratio) were prepared by suspending dry lipid films in deionized water by probe sonication at $70\ ^\circ\text{C}$ for 3 min. The vesicle suspensions were then cooled to room temperature, incubated overnight at $4\ ^\circ\text{C}$, and polymerized by irradiation at 254 nm for 30 s, resulting in solutions having an intense blue appearance. Small unilamellar vesicles (SUVs) composed of sphingomyelin, sphingomyelin/cholesterol (1/1 mol ratio), sphingomyelin/DMPG (9/1 mol ratio), and sphingomyelin/cholesterol/DMPG (4/5/1 mol ratio) were suspended in Hepes buffer (Hepes 10 mM, pH 7.4, NaN_3 0.02%) through probe sonication at $50\ ^\circ\text{C}$ for 10 min. Vesicle suspensions were centrifuged for 15 min at 6000g to remove any titanium particles.

Calcitonin Samples. Stock solutions of hCT were prepared by dissolving lyophilized peptide in filtered ($0.2\ \mu\text{m}$) deionized water at 1 mg/mL, followed by bath sonication on ice for 1 min. The stock solutions were aliquoted, immediately frozen, and stored at $-80\ ^\circ\text{C}$. The hCT solutions were diluted by Hepes buffer, mixed with appropriate vesicles (final lipid concentration 0.5 mM) or with Hepes buffer, and incubated at $26\ ^\circ\text{C}$ without agitation. Final hCT concentration was $64\ \mu\text{M}$. For control samples, deionized water was used instead of peptide stocks. Aliquots were withdrawn from the incubation mixtures at the indicated time-points and used for all experiments. Blocked Eppendorf tubes were used for incubation of the peptide solutions. The blocking was performed by shaking the tubes in a 3% skim milk powder dissolved in PBS (10 mM, pH 7.4) for 3 h at $37\ ^\circ\text{C}$. Subsequently, the tubes were washed under running distilled water and dried.

Lipid/Polydiacetylene (PDA) Chromatic Assay. At selected time points, $60\ \mu\text{L}$ aliquots were withdrawn from the peptide/PDA-based vesicles suspensions or from control vesicles samples that did not contain hCT. For experiments involving calcitonin fibrils grown in buffer, $30\ \mu\text{L}$ of the peptide samples containing hCT in Hepes buffer was added to equal volume of lipid/PDA vesicles, yielding $64\ \mu\text{M}$ calcitonin and 0.5 mM total lipid concentrations, respectively. The samples were mixed with $8\ \mu\text{L}$ of alamethicin (4 mg/mL in TFE/water 1/1), supplemented with $30\ \mu\text{L}$ of Tris-base buffer, 50 mM, pH 8, diluted by deionized water to 1 mL, and UV-vis spectra were acquired on a Jasco V-550 spectrophotometer (Jasco Corp., Tokyo). To quantify the extent of blue-to-red color transitions within the vesicle suspensions, the colorimetric response (% CR), was defined and calculated as follows:³⁶ $\% \text{ CR} = [(\text{PB}_0 - \text{PB}_1)/\text{PB}_0] \times 100\%$, in which $\text{PB} = A_{\text{blue}}/(A_{\text{blue}} + A_{\text{red}})$, where A_{blue} is the absorbance at 640 nm (the “blue” component of the spectrum), and A_{red} is the absorbance at 500 nm (the “red” component; “blue” and “red” refer to the visual appearance of the material, not actual absorbance). PB_0 is the blue/red ratio of the control sample before induction of a color change, and

PB_1 is the value obtained for the vesicle solution after the colorimetric transition has occurred. More reddish appearance of the vesicle suspensions indicates higher % CR values. $\Delta\text{CR}\%$ was calculated by subtracting % CR induced by alamethicin in PDA-containing vesicles from the corresponding values produced by alamethicin in vesicles/hCT mixtures.

Fluorescence Quenching Measurements. SUVs were prepared by the procedure described above. Prior to drying, the lipids were additionally supplemented with 1% NBD-PE. Aliquots of $15\ \mu\text{L}$ were taken from the incubation solutions containing lipid vesicles or hCT/vesicles mixtures and diluted by deionized water to 1 mL. The quenching reaction was initiated by adding sodium dithionite from a stock solution 0.6M, prepared in 50 mM Tris-base buffer, pH 11 to a final concentration of 0.6 mM. The decrease in fluorescence was recorded after 200 s incubation with the quencher using 468 nm excitation and 536 nm emission on FL920 spectrofluorimeter (Edinburgh, UK). The fluorescence decay calculated as a percentage of the initial fluorescence measured before the addition of dithionite.

Fluorescence Resonance Energy Transfer (FRET). SUVs were prepared by the procedure described above. Prior to drying, the lipids were additionally supplemented with NBD-PE and rhodamine-PE at a 100:1:1 molar ratio. At selected time points, $15\ \mu\text{L}$ aliquots were withdrawn from the incubation solutions containing lipid vesicles or hCT/vesicles suspensions, mixed with $4\ \mu\text{L}$ of alamethicin (4 mg/mL in TFE/water 1/1), diluted by deionized water to 0.5 mL, and fluorescence emission spectra were acquired on a FL920 spectrofluorimeter (Edinburgh, UK), applying an excitation wavelength of 469 nm. The percentage of FRET disruption was determined by the equation: $\% \text{ FRET disruption} = 100\% \times (R_i - R_0)/(R_{100\%} - R_0)$, where R is a ratio of fluorescence emissions NBD-PE (536 nm)/rhodamine-PE (590 nm), R_i indicates peptide/vesicles mixtures, $R_{100\%}$ was measured following the addition of 10% Triton X-100 to the vesicles (Triton X-100 is a detergent causing complete dissociation of the vesicles), and R_0 corresponds to vesicles without any additives. % FRET disruption of samples that did not contain alamethicin was subtracted from all measurements.

Thioflavin T (ThT) Fluorescence. Fibril formation was assessed by addition hCT solution in buffer or hCT/vesicles suspensions to ThT dissolved in Hepes buffer, resulting in $0.64\ \mu\text{M}$ hCT and $0.7\ \mu\text{M}$ ThT concentrations, respectively. ThT fluorescence was recorded using 440 nm excitation and 485 emission wavelengths on a FL920 spectrofluorimeter (Edinburgh, UK).

Transmission Electron Microscopy (TEM). Fibril/vesicles mixtures were visualized using $5\ \mu\text{L}$ of hCT/vesicles suspensions placed on 400 mesh copper grids covered with a carbon-stabilized Formvar film. Following 2 min incubation, excess solutions were removed and the grids were negatively stained for 1 min with a 1% uranyl acetate solution. Samples were viewed in JEOL 1200EX electron microscope operating at 120 kV.

Results

Calcitonin fibrillation was previously shown to accelerate in the presence of lipid bilayers, particularly membrane bilayers containing cholesterol.⁷ Our goal in this study was to determine whether, and to what extent, lipid-induced hCT aggregation affects the affinity and interactions of membrane-active peptides with the lipid bilayer. Figure 1 examines the relationship between lipid-induced hCT fibrillation and membrane interactions of the antimicrobial peptide alamethicin,^{24,26} which was added to the hCT/vesicle mixture at specific time points

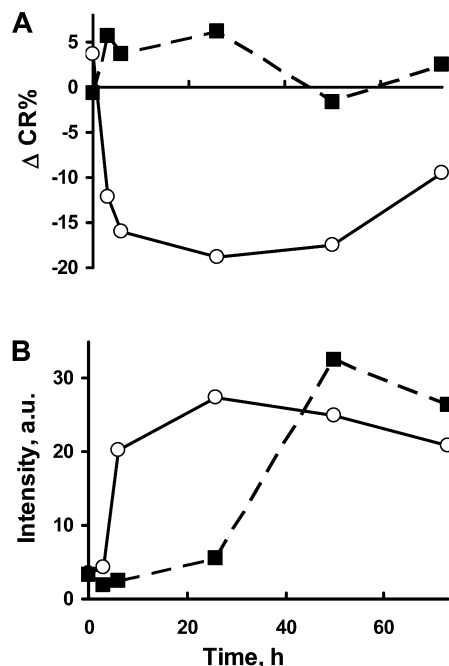


Figure 1. Inhibition of alamethicin–membrane interactions by hCT fibrillation. (A) Net colorimetric response (ΔCR) induced in lipid/PDA vesicles by alamethicin (difference between CR induced following addition of alamethicin to lipid/PDA vesicles preincubated with hCT, and alamethicin added to control lipid/PDA vesicles). (B) Fibrillation assay of hCT incubated with lipid/PDA vesicles: fluorescence emission of the fibril-binding dye ThT recorded in solutions comprising hCT and lipid/PDA vesicles having the following compositions: sphingomyelin/PDA (broken line), sphingomyelin/cholesterol/PDA (solid line).

throughout the incubation period. The extent of bilayer interactions was evaluated in Figure 1 through application of the lipid/polydiacetylene (PDA) vesicle assay.²⁸ PDA is a conjugated polymer undergoing visible colorimetric (blue–red) transformations induced by a variety of molecules which disrupt its conjugated framework.^{30,36–40} In particular, previous reports have shown that PDA embedded within lipid vesicles undergoes colorimetric transitions which are directly correlated to bilayer interactions of membrane-active peptides and other biomolecules.^{40–42} In essence, the PDA matrix in such biomimetic membrane vesicles constitutes a “chromatic reporter” of membrane binding events.³¹

Figure 1A shows the time evolution of the net chromatic response (ΔCR), defined as the difference between the CR (i.e., the colorimetric transformation of the lipid/PDA vesicles) induced by alamethicin which was added to lipid/PDA vesicles preincubated with hCT, and the CR induced by alamethicin added to control vesicles which were not incubated with hCT. Accordingly, the ΔCR values in Figure 1 essentially report whether preincubation of hCT with the lipid/PDA vesicles affected subsequent interactions of alamethicin with the biomimetic membranes; negative ΔCR thus indicate attenuation of alamethicin binding to the bilayer. The two lipid compositions represented in Figure 1 were designed to mimic components of the cellular membrane, particularly the lipid raft domains which comprise sphingomyelin and cholesterol, which were shown to significantly affect membrane interactions of amyloid proteins.^{43,44}

The colorimetric kinetic curves presented in Figure 1A demonstrate that incubation of hCT with vesicles comprising PDA, sphingomyelin, and cholesterol significantly attenuated the colorimetric transitions induced by alamethicin, i.e., resulted in negative ΔCR (Figure 1A, solid curve). In contrast, negligible effects upon alamethicin-induced color response (i.e., no inhibi-

tion of alamethicin–membrane interactions) were recorded, at all time points, when hCT was incubated with lipid/PDA vesicles which contained only sphingomyelin as the lipid component but no cholesterol (Figure 1A, broken curve). The chromatic results in Figure 1A thus indicate that incubation of hCT with sphingomyelin/cholesterol/PDA vesicles dramatically reduced bilayer interactions of alamethicin, while binding of alamethicin to sphingomyelin/PDA vesicles was not affected by preincubating the vesicles with hCT. Similar cholesterol-dependent inhibition of membrane interactions was recorded for other membrane-active peptides that are very different in their mechanisms of action (Supporting Information).

Lipid bilayers and cholesterol in particular have been previously shown to promote calcitonin fibrillation.^{7,22,23} Figure 1B examines the fibrillation kinetics of hCT in the presence of sphingomyelin/cholesterol/PDA vesicles and sphingomyelin/PDA vesicles, respectively, in order to determine whether a correlation exists between the attenuation of membrane interactions of alamethicin affected by hCT (Figure 1A), and hCT fibrillation. Indeed, the thioflavin-T (ThT) fluorescence curves in Figure 1B confirm that incubating hCT with the lipid/PDA vesicles promoted amyloid fibril formation, resulting in the increase in fluorescence of the fibril-bound ThT.^{45,46} In particular, the ThT fluorescence recorded in the presence of sphingomyelin/cholesterol/PDA vesicles (Figure 1B, solid curve) underscores a dramatic enhancement of hCT fibrillation, ascribed to the presence of cholesterol in the vesicles.⁷

A particularly important observation apparent in Figure 1 is the clear correlation between cholesterol-induced hCT fibrillation (solid curve in Figure 1B) and inhibition of membrane–alamethicin interactions (solid curve in Figure 1A). This correlation strongly suggests that cholesterol-induced fibrillation of hCT is the underlying cause for inhibition of alamethicin interactions with lipid bilayers. In contrast, while the ThT fluorescence data in Figure 1B indicate that prolonged incubation of hCT with sphingomyelin/PDA vesicles eventually led to fibrillation (Figure 1B, broken curve), hCT fibrillation in that case did not affect alamethicin–membrane interactions (Figure 1A, broken curve).

To complement and corroborate the data in Figure 1 indicating that cholesterol-induced hCT fibrillation modulated bilayer interactions of the membrane-active peptide alamethicin, we carried out additional experiments designed to characterize this apparent “bilayer shielding”. In particular, an important question one needs to address is whether hCT aggregates formed independently of the vesicle bilayers are capable of preventing membrane binding, or whether the fibrillation of hCT has to occur in the actual environment of the lipid bilayer in order to inhibit bilayer interactions of the membrane-active peptide.

Figure 2A depicts quantitative evaluation of the net CR (ΔCR) induced by alamethicin following addition to lipid/PDA vesicles to which hCT aggregates separately prepared in buffer were added. The experiment summarized in Figure 2 is fundamentally different from the assay depicted in Figure 1, in which hCT was preincubated with the lipid/PDA vesicles throughout the entire duration of the experiment. The ΔCR curves in Figure 2A clearly show that the hCT aggregates added to the lipid/PDA vesicles prior to alamethicin exerted negligible effects upon membrane interactions of the peptide. The absence of attenuation of alamethicin–membrane interactions by hCT, apparent in Figure 2 at all time points, stands in sharp contrast to the results depicted in Figure 1A which revealed the dramatic attenuation of alamethicin–bilayer binding when the vesicles contained cholesterol. Upon examination of the kinetic profile of fibril formation (ThT fluorescence results in Figure 2B), it is

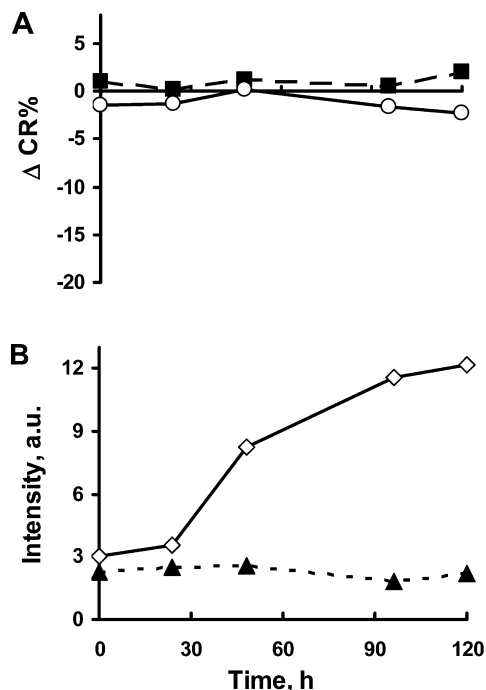


Figure 2. Independently formed hCT aggregates do not affect bilayer activity of alamethicin. (A) Net colorimetric response (ΔCR) induced by alamethicin was assayed following hCT incubation in buffer and subsequent addition to lipid/PDA vesicles containing sphingomyelin/PDA (broken line) or sphingomyelin/cholesterol/PDA (solid line). (B) Fluorescence emission of the fibril-binding dye ThT was recorded in a buffer solution containing hCT (solid line) or in control solution (no hCT, broken line).

clear that no effects upon membrane binding of alamethicin were apparent following addition of either the hCT monomers (present in the buffer solution in the initial time points) or oligomers (preceding the increase in ThT signal^{47,48} or the mature fibrils which formed after around 45 h in buffer and subsequently added to the lipid/PDA vesicles.

To corroborate the bilayer shielding phenomenon apparent in Figure 1, and to further characterize the cholesterol-dependent inhibition of alamethicin–membrane interactions, we carried out fluorescence resonance energy transfer (FRET) experiments, employing sphingomyelin and sphingomyelin/cholesterol vesicles, respectively, that additionally contained NBD-PE (fluorescence donor) and rhodamine-PE (fluorescence acceptor).³² FRET analysis has been routinely used to probe membrane interactions, since substances which bind to lipid bilayers generally modulate the FRET between membrane-embedded donor and acceptor.^{32,33,49} Figure 3 depicts the effect of preincubating hCT with the two vesicle types upon the FRET recorded after addition of alamethicin. Specifically, Figure 3 presents the difference between FRET measured after alamethicin addition to vesicles preincubated with hCT, and FRET determined upon alamethicin addition to control vesicles (which were not preincubated with hCT).

Like other membrane-active species, alamethicin disrupted the FRET upon interaction with the small unilamellar vesicles (SUVs, Figure 3A, broken line), due to an increase in the average distance between the vesicle-embedded fluorescence donor and acceptor.³³ However, similar to the lipid/PDA assay results in Figure 1, Figure 3 demonstrates that the presence of cholesterol in the vesicles resulted in significant reduction of the alamethicin-induced FRET disruption (Figure 3A, solid line). This outcome corresponds to lesser bilayer disruption by

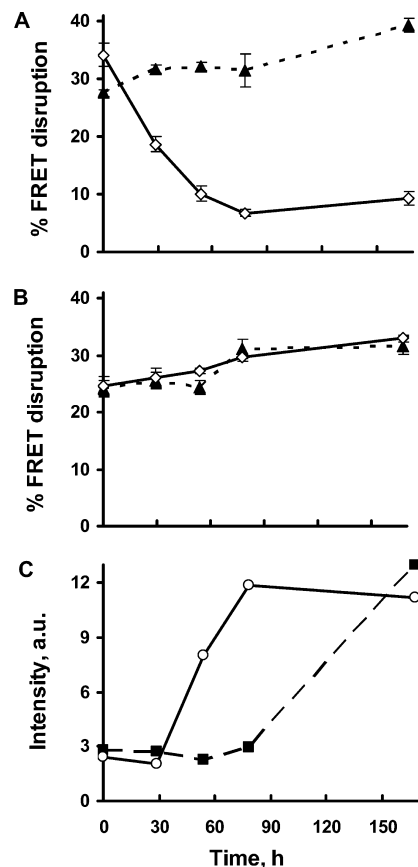


Figure 3. Inhibition of alamethicin–membrane interactions by hCT fibrils. (A,B) FRET disruption induced by alamethicin in small unilamellar vesicles (SUVs) that were preincubated with hCT (solid lines), and with control vesicles untreated with hCT (broken lines). Vesicles examined were (A) NBD-PE/rhodamine-PE/sphingomyelin/cholesterol; (B) NBD-PE/rhodamine-PE/sphingomyelin. (C) Fluorescence emission of the fibril-binding dye ThT recorded in the hCT/vesicle solutions: NBD-PE/rhodamine-PE/sphingomyelin/cholesterol (solid line); NBD-PE/rhodamine-PE/sphingomyelin (broken line).

alamethicin and correspondingly less impact on the average distance between the embedded donor and acceptor molecules. In contrast to the dramatic modulation of FRET by cholesterol-induced hCT fibrillation (Figure 3A), preincubation of hCT with sphingomyelin/NBD-PE/rhodamine-PE vesicles which did not contain cholesterol did not have any effect upon alamethicin interactions with the vesicles, i.e., the same FRET disruption as the control vesicle which were not preincubated with hCT (Figure 3B).

Overall, Figures 1–3 imply that the membrane shielding occurred only preincubation of hCT with cholesterol-containing bilayers, consequently leading to fibrillation and attenuation of binding to the lipid bilayers by membrane-active peptides such as alamethicin. To confirm that lipid bilayers were indeed directly involved in hCT fibrillation, we applied a fluorescence quenching assay³⁵ utilizing PG/sphingomyelin and PG/sphingomyelin/cholesterol vesicles, respectively, that further comprised NBD-PE, a fluorescent dye displayed on the vesicle surface (Figure 4).³⁴

Figure 4 depicts the time-dependent fluorescence emission of NBD-PE following addition of sodium dithionite, a water-soluble fluorescence quencher. In NBD-PE quenching experiments, binding of membrane-active species onto the vesicle surface generally results in a greater quenching of the NBD, since the dye which is localized at the lipid–water interface³⁴ becomes more exposed to the dithionite quencher in the aqueous

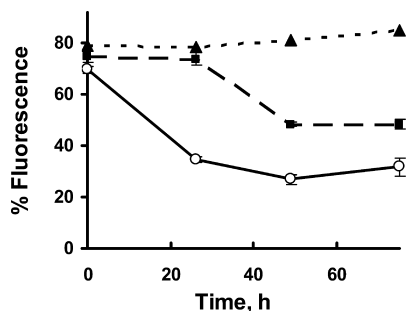


Figure 4. Fluorescence quenching experiments indicating that hCT interacts with bilayer vesicles. Interactions of hCT with the lipid bilayer surface were assessed by recording the quenching of NBD-PE fluorescence induced by the water-soluble quencher sodium dithionite in the control vesicles (short dashed), or in hCT/vesicle mixtures containing sphingomyelin/PG (long dashed), or sphingomyelin/cholesterol/PG (solid line).

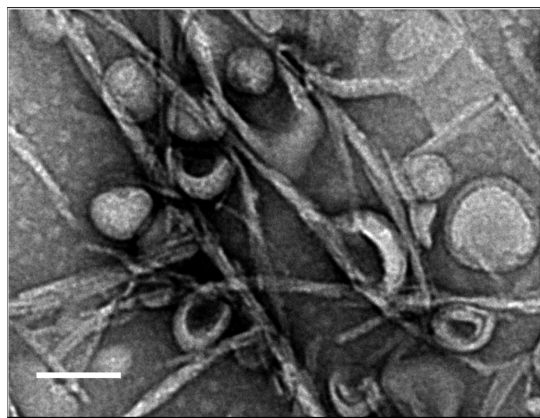


Figure 5. Electron microscopy of a hCT/vesicle mixture. The TEM image depicts hCT fibrils bound to sphingomyelin/cholesterol vesicles. The bar corresponds to 100 nm.

solution. Indeed, the results presented in Figure 4 demonstrate that incubation of hCT with lipid vesicles, particularly vesicles containing cholesterol (solid line in Figure 4), significantly enhanced the quenching of NBD compared to control vesicles (which were not preincubated with hCT). The data presented in Figure 4 confirm that the interactions between hCT and cholesterol-containing bilayers are the key factor contributing to hCT fibrillation, which consequently resulted in inhibition of alamethicin-membrane interactions (Figures 1–3).

Figure 5 shows a representative transmission electron microscopy (TEM) image providing visual depiction of the bilayer-associated hCT fibrillar species. The TEM image in Figure 5, which corresponds to hCT incubated for 48 h with sphingomyelin/cholesterol vesicles, shows elongated hCT fibrils colocalized and highly intertwined with the lipid vesicles. Furthermore, the TEM image indicates that the vesicles appear enveloped by fiber fragments, consistent with the results of the biophysical techniques presented above.

Discussion

The realization that membrane interactions of amyloidogenic proteins play major roles in amyloid diseases underscores the intense efforts to characterize and elucidate the mechanisms of amyloid-associated membrane events. Experimental evidence increasingly appears to indicate that oligomeric species formed at early stages of amyloid peptide aggregation, rather than mature full length fibrils, play the primary role in amyloid-induced cytotoxicity.^{50–54} Moreover, varied reports have indi-

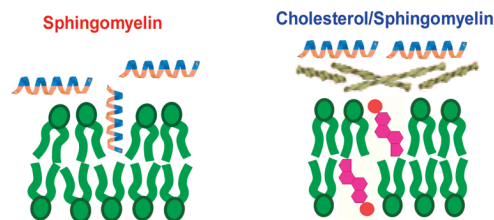


Figure 6. Schematic description of the membrane shielding phenomenon. Membrane-active molecules (helical peptides in the figure) penetrate into the bilayer containing sphingomyelin (green). However, in the presence of cholesterol molecules (purple), calcitonin fibrils (gray) assemble at the bilayer surface, effectively preventing interactions by the peptides.

cated that fibril aggregates by themselves might not be responsible for disease pathologies; amyloid plaques were detected, for example, in brains of individuals unaffected by amyloid disorders.⁵⁵ Furthermore, neurons containing fibrillar inclusions incriminated in Huntington's disease exhibited improved survival compared to their counterparts lacking fibrillar aggregates.⁵⁶ Rapid fibrillation was also shown to protect from cognitive decline mice overexpressing a human β -amyloid protein.⁵² These and other studies suggest that extensive fibrillation might actually protect cells by eliminating transient oligomeric species.

The experiments described here reveal an intriguing phenomenon, in which fibrillation of human calcitonin in the presence of lipid bilayers containing cholesterol results in a “shielding layer”, effectively inhibiting binding and bilayer insertion of membrane-active peptides (Figure 6). The shielding effect, schematically depicted in Figure 6, appears to be generic and has been observed in case of different membrane-active biomolecules in addition to alamethicin, including melittin, valinomycin, and histone (Supporting Information). The observation of calcitonin-induced bilayer shielding for peptides exhibiting different membrane interaction mechanisms strongly suggest that the effect is nonspecific, e.g., do not depend upon particular bilayer insertion mechanism (such as channel formation in case of alamethicin).

The biophysical and microscopy experiments carried out demonstrated the close interplay between lipid membranes containing cholesterol and fibrillation of hCT, which correlates with the observed bilayer shielding. The lipid/PDA vesicle assay experiments (Figures 1) clearly showed that hCT fibrillation in the presence of cholesterol-containing vesicles resulted in attenuation of membrane binding by alamethicin, a membrane-active peptide. Consistent with the chromatic membrane assay, FRET results (Figure 3) showed that hCT fibrillation significantly affected the modulation of energy transfer between bilayer-embedded fluorescence donor and acceptor induced by alamethicin. NBD fluorescence quenching analysis (Figure 4) confirmed that interactions of hCT with the bilayer surface were strongly correlated with fibrillation of the peptide, underlining the link between the bilayers and the assembled hCT fibrils. Electron microscopy additionally showed that hCT fibrils were associated with cholesterol-containing lipid vesicles without disrupting their integrity and structure.

The experiments highlight two important features pertaining to the membrane shielding phenomenon. First, the effect is observed only when fibrillation is carried out in the presence of the lipid bilayers; as shown in Figure 2, fibrillar species that were separately formed and only then added to the vesicles did not produce any effect upon the lipid bilayers. Second, while varied lipids were shown to accelerate hCT fibrillation, we find

that cholesterol is the pivotal molecule within the bilayers which generated the observed shielding effect. Cholesterol, the primary component of lipid raft domains within the plasma membrane, has indeed been implicated in numerous amyloidogenic processes.^{43,57} A likely function for cholesterol in promoting membrane shielding is through targeting of the assembled fibrils onto the bilayer surface.

While the exact mechanism for the calcitonin-induced bilayer shielding is not entirely clear at this point, two possible scenarios emerge. One possibility is that interaction of the fibrillar species with the lipid bilayer induces long-range rearrangement of the lipid molecules within the bilayer, consequently limiting the accommodation of external peptides and their membrane internalization. An alternative description is that calcitonin creates interspersed network closer to the bilayer surface, thereby blocking binding of membrane-active substances. Indeed, we believe that the latter situation is more likely to occur, due to the generic nature of the shielding phenomena for diverse biomolecules (Supporting Information).

Conclusions

This work presents evidence that lipid-induced fibrils formed by the amyloidogenic protein human calcitonin block membrane binding and insertion of alamethicin, a membrane-active antibiotic peptide. This “membrane-shielding” effect was observed only when the bilayer vesicles contained cholesterol, pointing to a possible role of the sterol of docking the fibril network onto the membrane surface. This study may point to a putative protection mechanism in which membrane-associated fibrillation prevents bilayer disruption by toxic oligomeric amyloid species. The new phenomenon might represent a novel mechanism for protection, rather than disruption, of cellular membranes by amyloid proteins.

Supporting Information Available: Inhibition of additional membrane-active compounds by hCT fibrils. This material is available free of charge via the Internet at <http://pubs.acs.org>.

References and Notes

- (1) Arispe, N.; Diaz, J. C.; Simakova, O. *Biochim. Biophys. Acta* **2007**, *1768*, 1952–65.
- (2) Arispe, N.; Pollard, H. B.; Rojas, E. *Proc. Natl. Acad. Sci. U.S.A.* **1993**, *90*, 10573–7.
- (3) Lashuel, H. A.; Hartley, D.; Petre, B. M.; Walz, T.; Lansbury, P. T., Jr. *Nature* **2002**, 418–291.
- (4) Lashuel, H. A.; Lansbury, P. T., Jr. *Q. Rev. Biophys.* **2006**, *39*, 167–201.
- (5) Gorbenko, G. P.; Kinnunen, P. K. *Chem Phys Lipids* **2006**, *141*, 72–82.
- (6) Vestergaard, M.; Hamada, T.; Takagi, M. *Biotechnol. Bioeng.* **2008**, *99*, 753–63.
- (7) Wang, S. S.; Good, T. A.; Rymer, D. L. *Int. J. Biochem. Cell Biol.* **2005**, *37*, 1656–69.
- (8) Bokvist, M.; Lindstrom, F.; Watts, A.; Grobner, G. *J. Mol. Biol.* **2004**, *335*, 1039–49.
- (9) MacIntyre, I. *Calcif. Tissue Res.* **1967**, *1*, 173–82.
- (10) Mehta, N. M.; Malootian, A.; Gilligan, J. P. *Curr. Pharm. Des.* **2003**, *9*, 2659–76.
- (11) Kanis, J. A.; Horn, D. B.; Scott, R. D.; Strong, J. A. *Br. Med. J.* **1974**, *3*, 727–31.
- (12) Arvinte, T.; Cudd, A.; Drake, A. F. *J. Biol. Chem.* **1993**, *268*, 6415–6422.
- (13) Khurana, R.; Agarwal, A.; Bajpai, V. K.; Verma, N.; Sharma, A. K.; Gupta, R. P.; Madhusudan, K. P. *Endocrinology* **2004**, *145*, 5465–70.
- (14) Sletten, K.; Westermarck, P.; Natvig, J. B. **1976**, *143*, p 993–998.
- (15) Berger, G.; Berger, N.; Guillaud, M. H.; Trouillas, J.; Vauzelle, J. L. *Virchows Arch. A Pathol. Anat. Histopathol.* **1988**, *412*, 543–51.
- (16) Silver, M. M.; Hearn, S. A.; Lines, L. D.; Troster, M. *J. Histochem. Cytochem.* **1988**, *36*, 1031–6.
- (17) Fragu, P. *Gesnerus* **2007**, *64*, 69–92.
- (18) Wimalawansa, S. J. *Mol. Cell. Endocrinol.* **1990**, *71*, 13–9.
- (19) Avidan-Shpalter, C.; Gazit, E. *Amyloid* **2006**, *13*, 216–25.
- (20) Diociaiuti, M.; Polzi, L. Z.; Valvo, L.; Malchiodi-Albedi, F.; Bombelli, C.; Gaudiano, M. C. *Biophys. J.* **2006**, *91*, 2275–81.
- (21) Stipani, V.; Gallucci, E.; Micelli, S.; Picciarelli, V.; Benz, R. *Biophys. J.* **2001**, *81*, 3332–8.
- (22) Hui, S. W.; Epand, R. M.; Dell, K. R.; Epand, R. F.; Orlowski, R. C. *Biochim. Biophys. Acta* **1984**, *772*, 264–72.
- (23) Wagner, K.; Van Mau, N.; Boichot, S.; Kajava, A. V.; Krauss, U.; Le Grimmellec, C.; Beck-Sickinger, A.; Heitz, F. *Biophys. J.* **2004**, *87*, 386–395.
- (24) Bechinger, B. *J. Membr. Biol.* **1997**, *156*, 197–211.
- (25) He, K.; Ludtke, S. J.; Heller, W. T.; Huang, H. W. *Biophys. J.* **1996**, *71*, 2669–2679.
- (26) Marsh, D. *Biochemistry* **2009**, *48*, 729–37.
- (27) Volinsky, R.; Kolusheva, S.; Berman, A.; Jelinek, R. *Biochim. Biophys. Acta* **2006**, *1758*, 1393–407.
- (28) Jelinek, R.; Kolusheva, S. *Biotechnol. Adv.* **2001**, *19*, 109–18.
- (29) Kolusheva, S.; Boyer, L.; Jelinek, R. *Nat. Biotechnol.* **2000**, *18*, 225–7.
- (30) Kolusheva, S.; Kafri, R.; Katz, M.; Jelinek, R. *J. Am. Chem. Soc.* **2001**, *123*, 417–22.
- (31) Kolusheva, S.; Wachtel, E.; Jelinek, R. *J. Lipid Res.* **2003**, *44*, 65–71.
- (32) Lakowicz, J. R. In *Principles of fluorescence spectroscopy*, 3rd ed.; Kluwer Academic/ Plenum Publishers: New York, 2006; pp 443–472.
- (33) Wilschut, J.; Scholma, J.; Eastman, S. J.; Hope, M. J.; Cullis, P. R. *Biochemistry* **1992**, *31*, 2629–36.
- (34) Lakowicz, J. R. In *Principles of fluorescence spectroscopy*, 3rd ed.; Kluwer Academic/ Plenum Publishers: New York, 2006; pp 278–327.
- (35) McIntyre, J. C.; Sleight, R. G. *Biochemistry* **1991**, *30*, 11819–27.
- (36) Jelinek, R.; Okada, S.; Norvez, S.; Charych, D. *Chem. Biol.* **1998**, *5*, 619–29.
- (37) Charych, D. H.; Nagy, J. O.; Spevak, W.; Bednarski, M. D. *Science* **1993**, *261*, 585–588.
- (38) Katz, M.; Ben-Shlush, I.; Kolusheva, S.; Jelinek, R. *Pharm. Res.* **2006**, *23*, 580–8.
- (39) Kolusheva, S.; Molt, O.; Herm, M.; Schrader, T.; Jelinek, R. *J. Am. Chem. Soc.* **2005**, *127*, 10000–1.
- (40) Porat, Y.; Kolusheva, S.; Jelinek, R.; Gazit, E. *Biochemistry* **2003**, *42*, 10971–7.
- (41) Kolusheva, S.; Friedman, J.; Angel, I.; Jelinek, R. *Biochemistry* **2005**, *44*, 12077–85.
- (42) Kolusheva, S.; Shahal, T.; Jelinek, R. *Biochemistry* **2000**, *39*, 15851–9.
- (43) Fantini, J.; Garmy, N.; Mahfoud, R.; Yahi, N. *Expert Rev. Mol. Med.* **2002**, *4*, 1–22.
- (44) Mahfoud, R.; Garmy, N.; Maresca, M.; Yahi, N.; Puigserver, A.; Fantini, J. *J. Biol. Chem.* **2002**, *277*, 11292–6.
- (45) LeVine, H., 3rd. *Protein Sci* **1993**, *2*, 404–10.
- (46) Khurana, R.; Coleman, C.; Ionescu-Zanetti, C.; Carter, S. A.; Krishna, V.; Grover, R. K.; Roy, R.; Singh, S. *J. Struct. Biol.* **2005**, *151*, 229–38.
- (47) Fink, A. L. *Acc. Chem. Res.* **2006**, *39*, 628–34.
- (48) Smith, A. M.; Jahn, T. R.; Ashcroft, A. E.; Radford, S. E. *J. Mol. Biol.* **2006**, *364*, 9–19.
- (49) Glaser, P. E.; Gross, R. W. *Biochemistry* **1994**, *33*, 5805–12.
- (50) Bucciantini, M.; Giannoni, E.; Chiti, F.; Baroni, F.; Formigli, L.; Zurdo, J.; Taddei, N.; Ramponi, G.; Dobson, C. M.; Stefani, M. *Nature* **2002**, *416*, 507–511.
- (51) Coughney, B.; Lansbury, P. T. *Annu. Rev. Neurosci.* **2003**, *26*, 267–298.
- (52) Cheng, I. H.; Searce-Levie, K.; Legleiter, J.; Palop, J. J.; Gerstein, H.; Bien-Ly, N.; Puolivali, J.; Lesne, S.; Ashe, K. H.; Muchowski, P. J.; Mucke, L. *J. Biol. Chem.* **2007**, *282*, 23818–28.
- (53) Kaye, R.; Head, E.; Thompson, J. L.; McIntire, T. M.; Milton, S. C.; Cotman, C. W.; Glabe, C. G. *Science* **2003**, *300*, 486–489.
- (54) Lesne, S.; Koh, M. T.; Kotilinek, L.; Kaye, R.; Glabe, C. G.; Yang, A.; Gallagher, M.; Ashe, K. H. *Nature* **2006**, *440*, 352–7.
- (55) Klein, W. L.; Krafft, G. A.; Finch, C. E. *Trends Neurosci.* **2001**, *24*, 219–24.
- (56) Arrasate, M.; Mitra, S.; Schweitzer, E. S.; Segal, M. R.; Finkbeiner, S. *Nature* **2004**, *431*, 805–10.
- (57) Yanagisawa, K.; Matsuzaki, K. *Ann. N.Y. Acad. Sci.* **2002**, *977*, 384–6.